Comparison of K^+ and e^- Quasielastic Scattering

J. Piekarewicz

Supercomputer Computations Research Institute, Florida State University, Tallahassee FL 32306

J. R. Shepard

Department of Physics, University of Colorado, Boulder, CO 80309-0446

We formulate K^+-nucleus quasielastic scattering in a manner which closely parallels standard treatments of e^--nucleus quasielastic scattering. For K^+ scattering, new responses involving scalar contributions appear in addition to the Coulomb (or longitudinal) and transverse (e, e') responses which are of vector character. We compute these responses using both nuclear matter and finite nucleus versions of the Relativistic Hartree Approximation to Quantum Hadrodynamics including RPA correlations. Overall agreement with measured (e, e') responses and new K^+ quasielastic scattering data for ^{40}Ca at $|\mathbf{q}| = 500$ MeV/c is good. Strong RPA quenching is essential for agreement with the Coulomb response. This quenching is notably less for the K^+ cross section even though the new scalar contributions are even more strongly quenched than the vector contributions. We show that this "differential quenching" alters sensitive cancellations in the expression for the K^+ cross section so that it is reduced much less than the individual responses. We emphasize the role of the purely relativistic distinction between vector and scalar contributions in obtaining an accurate and consistent description of the (e, e') and K^+ data within the framework of our nuclear structure model.

arXiv:nucl-th/9408021v1 18 Aug 1994

I. INTRODUCTION

Quasielastic electron scattering from nuclei has long been used to study various aspects of nuclear structure. The strong quenching of the measured Coulomb response relative to Fermi gas estimates is one prominent example [1,2,3]. Such studies are facilitated by (1) the (reasonably) well-understood nature of the fundamental eN interaction and (2) by the relative weakness of that interaction. However, this same interaction suffers from some important shortcomings in that it probes the nucleus in a very restricted fashion. Hence only two independent observables exist (without making polarization measurements), namely the Coulomb (or longitudinal) and transverse responses. These limitations have motivated a number of quasielastic scattering experiments employing hadronic probes [4,5,6,7] . The more complicated interaction of the probe with nucleons means that – in principle – new responses which are inaccessible with electrons can be studied. One important example of such investigations is found in the $(\vec{p}, \vec{p}')$ (Refs. [4,5]) and $(\vec{p}, \vec{n})$ (Refs. [6]) experiments performed (in part) to extract the *longitudinal* spin response to complement information on the transverse spin response determined by electron scattering. Analysis of such hadronic measurements is, however, hampered by the strength and complexity of the projectile- nucleon interaction. The former causes strong distortions in the incoming and outgoing projectile wavefunctions and localizes the scattering process in the region of the nuclear surface. The latter typically implies significant modification of the interaction in the nuclear medium. Both sets of effects greatly complicate the theoretical description of the scattering process and the extraction of nuclear structure information.

These considerations have led to much interest in K^+-nucleus scattering. The relative weakness of the K^+N interaction relative to, *e.g.*, NN and πN interactions suggests that distortions and medium effects may be simpler to handle and that the scattering process may be more sensitive to the nuclear interior. Estimates of the mean-free-paths (MFP's) of the various probes support the latter assertion. For example, at a laboratory momentum of 700 MeV/c, the proton and the π^+ have MFP's of about 2 fm while the K^+ MFP is roughly twice that value.

While K^+-nucleus scattering experiments are still in their infancy, their promise has been some what diminished by early results. In particular, there is a persistant discrepancy between measured K^+-nucleus elastic and total cross sections and theoretical results based on multiple scattering models which are expected to be accurate due again to the weakness of the K^+N interaction [8].

Data for K^+-nucleus quasielastic scattering from C, Ca and Pb at a laboratory K^+ momentum of 705 MeV/c have recently become available [9,10] . A preliminary theoretical analysis of the $|\mathbf{q}|=$ 300 and 500 MeV/c data for ^{12}C and ^{40}Ca has already appeared along with the data [9]. In the present paper, we extend those preliminary calculations and focus on comparison with ^{40}Ca(e, e') data at $|\mathbf{q}| =$ 500 MeV/c. In so doing, we make the first attempt to realize the promise of K^+ scattering to provide nuclear structure information complementary to that extracted from electron data. The remainder of this paper is organized as follows: in Section II, we derive well known results for (e, e') quasielastic scattering so as to establish a framework for treating K^+ scattering which is addressed in Section III. Section IV touches upon problems associated with ambiguities in the forms of both the eN and K^+N on-shell elastic scattering amplitudes. Past efforts to resolve the eN ambiguity

are summarized and a resolution for K^+N is proposed. The theoretical treatment of nuclear structure is outlined in Section V. Specific calculations of electron and K^+ cross sections and comparisons with data appear in Section VI where it is shown that, due to details of the structure of the K^+ quasielastic cross section, the strong quenching observed for the (e, e') Coulomb response does *not* appear for the K^+ process even though the latter is dominated by a contribution which is superficially very similar to the Coulomb response. Section VII contains a summary of the present work and our conclusions.

II. FORMALISM FOR ELECTRON-NUCLEUS SCATTERING

The discussion of electron scattering from nucleons and nuclei presented in this section is considerably more detailed than would seem warranted given that no new results appear. However, this detail is supplied so as to provide a familiar context for developing our treatment of K^+ scattering which will be outlined in Section III.

The unpolarized e^- scattering differential cross section in plane wave Born approximation is

$$d\sigma = \frac{1}{v_{rel}} \frac{4\alpha^2}{(q^2)^2} \, \ell_{\mu\nu} \, W_{EM}^{\mu\nu} \, d^3p_f \tag{1}$$

where $q = p_i - p_f = (\omega, \mathbf{q})$ and $p_i = (\epsilon_i, \mathbf{p}_i)$, $p_f = (\epsilon_f, \mathbf{p}_f)$ are the initial and final electron 4-momenta, respectively, and the electron electromagnetic tensor is

$$\begin{aligned} \ell_{\mu\nu} &= \frac{1}{2} \sum_{s_f s_i} \text{Tr}\left[\gamma_\mu \, u(p_f s_f)\bar{u}(p_f s_f) \, \gamma_\nu \, u(p_i s_i)\bar{u}(p_i s_i)\right] \\ &= \frac{1}{\epsilon_f \epsilon_i} \left[p_\mu p_\nu + \frac{1}{4}(q^2 g_{\mu\nu} - q_\mu q_\nu)\right] \end{aligned} \tag{2}$$

where $p = \frac{1}{2}(p_i + p_f)$ and, *e.g.*,

$$u(p_i, s_i) = \sqrt{\frac{\epsilon_i + m}{2\epsilon_i}} \left(\begin{array}{c} 1 \\ \frac{\sigma \cdot \mathbf{p}_i}{\epsilon_i + m} \end{array}\right) \chi(s_i) \tag{3}$$

where m is the electron mass. Also,

$$W_{EM}^{\mu\nu} = -\frac{1}{\pi} \, \text{Im} \, \Pi_{EM}^{\mu\nu}(\mathbf{q}, \mathbf{q}; \omega) \tag{4}$$

is the electromagnetic response of the scatterer. For nuclear scattering,

$$\Pi_{EM}^{\mu\nu}(\mathbf{q}, \mathbf{q}'; \omega) \equiv \int d^3y \, e^{-i\mathbf{q}\cdot\mathbf{y}} \int d^3y' \, e^{+i\mathbf{q}'\cdot\mathbf{y}'} \, \Pi_{EM}^{\mu\nu}(\mathbf{y}, \mathbf{y}'; \omega) \tag{5}$$

where the polarization insertion $\Pi_{EM}^{\mu\nu}(\mathbf{y}, \mathbf{y}'; \omega)$ is defined via

$$\begin{aligned} \Pi_{EM}^{\mu\nu}(y, y') &\equiv \frac{1}{i} < i|T[\hat{\bar{\psi}}(y)\Gamma_{EM}^\mu\hat{\psi}(y) \, \hat{\bar{\psi}}(y')\Gamma_{EM}^\nu\hat{\psi}(y')]|i> \\ &= \int \frac{d\omega}{2\pi} \, e^{-i\omega(y_0 - y_0')} \, \Pi_{EM}^{\mu\nu}(\mathbf{y}, \mathbf{y}'; \omega). \end{aligned} \tag{6}$$

3

In these expressions, the nucleon electromagnetic current operator is

$$\Gamma^\mu_{EM} \equiv F_1(q^2)\gamma^\mu + iF_2(q^2)\frac{\sigma^{\mu\nu}(P_f - P_i)_\nu}{2M} \tag{7}$$

where M is the nucleon mass and P_i (P_f) is the initial (final) nucleon momentum.

We now consider e-nucleon scattering. It is useful to recall the Lehmann representation of the polarization insertion which implies, *e.g.*,

$$-\frac{1}{\pi} \text{ Im } \Pi^{\mu\nu}_{EM}(\mathbf{q}, \mathbf{q}; \omega) = \sum_f (J^\mu_{fi})^* J^\nu_{fi} \quad \delta(\omega - E_f + E_i) \tag{8}$$

where

$$J^\mu_{fi} = \int d^3y \; e^{+i\mathbf{q}\cdot\mathbf{y}} \; < f|\hat{\bar{\psi}}(\mathbf{y}) \; \Gamma^\mu_{EM} \; \hat{\psi}(\mathbf{y})|i> . \tag{9}$$

For a single nucleon, J^μ_{fi} is readily evaluated and we find

$$W^{\mu\nu}_{EM} \to \delta(\omega - E_f + E_i) \; \delta_{\mathbf{q},\mathbf{P}_f-\mathbf{P}_i} \; \ell^{\mu\nu}(N) \tag{10}$$

where the Kroenecker δ comes from the box normalization of the free nucleon wavefunction and where the *nucleon* electromagnetic tensor is

$$\ell^{\mu\nu}(N) \equiv \frac{1}{2} \sum_{S_f S_i} \text{ Tr } \left[\Gamma^\mu_{EM} \; u(P_f S_f)\bar{u}(P_f S_f) \; \Gamma^\nu_{EM} \; u(P_i S_i)\bar{u}(P_i S_i) \right]$$

$$\to \frac{1}{E_f E_i} \left[\frac{G^2_E + \tau G^2_M}{1 + \tau} \; P^\mu P^\nu + G^2_M \; \frac{1}{4}(q^2 g^{\mu\nu} - q^\mu q^\nu) \right] \tag{11}$$

with $P \equiv \frac{1}{2}(P_f + P_i)$, $\tau \equiv -q^2/4M^2 = Q^2/4M^2$ and Sach's form factors, $G_M = F_1 + F_2$ and $G_E = F_1 - \tau F_2$.

Then, in the initial nucleon rest frame, using $p \equiv |\vec{p}|$,

$$\frac{d\sigma}{d\Omega}\Big|_{lab} = \int_{0^+}^\infty \frac{\epsilon_i}{p_i} \frac{4\alpha}{(q^2)^2} \; \ell_{\mu\nu} \; \ell^{\mu\nu}(N) \; \delta(\epsilon_i - \epsilon_f + E_i - E_f) \; \delta_{\mathbf{p}_i-\mathbf{p}_f,\mathbf{P}_f-\mathbf{P}_i} \; p^2_f dp_f. \tag{12}$$

Evaluating the integral *at fixed scattering angle* yields

$$\frac{d\sigma}{d\Omega}\Big|_{lab} = \frac{4\alpha}{(q^2)^2} \; \ell_{\mu\nu} \; \ell^{\mu\nu}(N) \; \frac{\epsilon_i}{p_i} \; \frac{p_f E_f}{\left| p_f(\epsilon_i + M) - \epsilon_f p_i \cos\theta \right|} \; p_f\epsilon_f \tag{13}$$

where we now understand that p_f, ϵ_f and E_f take on their on-shell values in the final state.

For an infinitely massive structureless proton, $\tau \to 0$, $E_f \to M$, $p_f = p_i$, $\epsilon_f = \epsilon_i$ and $F_1 \to 1$, $F_2 \to 0$ which implies $G^E, G^M \to 1$. In this limit,

$$\ell^{\mu\nu}(N) \to g^{\mu 0}g^{\nu 0} \tag{14}$$

and

$$q^2 = -\mathbf{q}^2 = -4p^2_i \sin\theta/2. \tag{15}$$

We then have

$$\frac{d\sigma}{d\Omega}\bigg|_{lab} \to \sigma_M = \frac{\alpha^2}{4\beta^2 p_i^2 \sin^4\theta/2} \, (1 - \beta^2 \sin^2\theta/2) \tag{16}$$

which is the Mott cross section. For ultrarelativistic electrons, this expression becomes

$$\sigma_M \to \sigma_M' = \frac{\alpha^2 \, \cos^2\theta/2}{4\epsilon_i^2 \sin^4\theta/2}. \tag{17}$$

For physical nucleons; *i.e.*, when no approximation to $\ell^{\mu\nu}(N)$ is made, we find, for ultrarelativistic electrons, the familiar result

$$\frac{d\sigma}{d\Omega}\bigg|_{lab} = \sigma_M' \left(1 - \frac{2\tau M}{\epsilon_i}\right) \left[\frac{G_E^2 + \tau G_M^2}{1 + \tau} + 2\tau G_M^2 \tan^2\theta/2\right]. \tag{18}$$

Next, we examine e-nucleus scattering. Using $pdp = \epsilon d\epsilon$, Eq. 1 yields, in the nuclear rest frame,

$$\frac{d^2\sigma}{d\omega d\Omega} = \frac{4\alpha^2}{(q^2)^2} \frac{\epsilon_i p_f \epsilon_f}{p_i} \, \ell_{\mu\nu} W_{EM}^{\mu\nu} \tag{19}$$

Using the fact that $q_\mu W_{EM}^{\mu\nu} = q_\nu W_{EM}^{\mu\nu} = 0$ due to current conservation, we find

$$\frac{d^2\sigma}{d\omega d\Omega} = \frac{4\alpha^2}{(q^2)^2} \frac{p_f}{p_i} \, m^2 \, \left\{ \left(\frac{\epsilon_f + \epsilon_i}{2m}\right)^2 \left[\left(\frac{Q^2}{\mathbf{q}^2}\right)^2 W_{EM}^{00} + \frac{Q^2}{\mathbf{q}^2} W_{EM}^{11}\right] \right.$$
$$- \left(1 + \frac{Q^2}{4m^2}\right) W_{EM}^{11}$$
$$\left. - \frac{Q^2}{4m^2} \frac{Q^2}{\mathbf{q}^2} \, W_{EM}^{00} + \frac{Q^2}{2m^2} \, W_{EM}^{11} \right\}. \tag{20}$$

For ultrarelativistic electrons this reduces to the familiar expression [12]

$$\frac{d^2\sigma}{d\omega d\Omega} = \sigma_M' \left[\left(\frac{Q^2}{\mathbf{q}^2}\right)^2 W_{EM}^{00} + \left(\frac{Q^2}{2\mathbf{q}^2} + \tan^2\theta/2\right) 2W_{EM}^{11}\right] \tag{21}$$

in which we identify the Coulomb and transverse responses, namely, $W_C = W_{EM}^{00}$ and $W_T = 2W_{EM}^{11}$, respectively. We now observe that the expression for the ultrarelativistic eN cross section in the initial nucleon rest frame (Eq. 18) can be expressed as

$$\frac{d\sigma}{d\Omega}(eN) = \int \, d\omega \, \frac{d^2\sigma}{d\omega d\Omega}(eN)\bigg|_{\text{fixed angle}} \tag{22}$$

where

$$\frac{d^2\sigma}{d\omega d\Omega}(eN) = \sigma_M' \, \delta(\omega - E_f + M) \, \delta_{\mathbf{q},\mathbf{P}_f}$$
$$\times \left[\left(\frac{Q^2}{\mathbf{q}^2}\right)^2 \frac{1 + \tau}{1 + 2\tau} G_E^2 + \left(\frac{Q^2}{2\mathbf{q}^2} + \tan^2\theta/2\right) 2 \, \frac{\tau}{1 + 2\tau} G_M^2\right]. \tag{23}$$

Comparison with Eq. 21 allows us to determine the *single nucleon* electromagnetic responses

$$W_{EM}^{00} \to W_{EM}^{00}(N) = \delta(\omega - E_f + M) \, \delta_{\mathbf{q},\mathbf{P}_f} \frac{1 + \tau}{1 + 2\tau} G_E^2, \tag{24}$$

$$W_{EM}^{11} \to W_{EM}^{11}(N) = \delta(\omega - E_f + M) \, \delta_{\mathbf{q},\mathbf{P}_f} \frac{\tau}{1 + 2\tau} G_M^2. \tag{25}$$

These expressions also follow directly from Eq. 9 when applied to a free nucleon.

III. FORMALISM FOR KAON-NUCLEUS SCATTERING

This section presents a treatment of K^+N and K^+-nucleus scattering which emphasizes the relation to the formulation of e^- scattering appearing in the previous section. We begin by considering the (fictitious) scattering of a K^+ which interacts only electromagnetically with the scatterer. (Alternatively, we can think of the scattering of a "spinless electron".) Using arguments analogous to those which led to Eq. 1 in Section II, we find that the K^+ *electromagnetic* cross section is given in plane wave Born approximation by

$$d\sigma = \frac{1}{v_{rel}} \frac{4\alpha^2}{(q^2)^2} L_{\mu\nu} W_{EM}^{\mu\nu} d^3 p_f \tag{26}$$

where now $q = p_i - p_f$ where p_i and p_f are the initial and final K^+ momenta and $L_{\mu\nu}$ is the K^+ electromagnetic tensor given by

$$
\begin{aligned}
L_{\mu\nu} &= \frac{1}{4\epsilon_f \epsilon_i} (p_i + p_f)_\mu (p_i + p_f)_\nu \\
&= \frac{1}{\epsilon_f \epsilon_i} p_\mu p_\nu.
\end{aligned}
\tag{27}
$$

This expression is to be compared with the electron electromagnetic tensor, Eq. 2. Differences are clearly due to the presence of "spin currents" in the electron case.

We now treat K^+N electromagnetic scattering. It is simple to show that, in analogy with Eq. 13,

$$\frac{d\sigma}{d\Omega}(K^+N - EM)\Big|_{lab} = \frac{4\alpha}{(q^2)^2} L_{\mu\nu} \ell^{\mu\nu}(N) \frac{\epsilon_i}{p_i} \frac{p_f E_f}{\left| p_f(\epsilon_i + M) - \epsilon_f p_i \cos\theta \right|} p_f \epsilon_f. \tag{28}$$

For a massive structureless proton, we have

$$\frac{d\sigma}{d\Omega}(K^+N - EM)\Big|_{lab} \rightarrow \frac{\alpha^2}{4\beta^2 p_i^2 \sin^4 \theta/2} \tag{29}$$

which should be compared with the Mott cross section appearing in Eq. 16. (Since the limit of ultrarelativistic K^+'s is irrelevant for the measurements to be discussed below, we do not present the corresponding formulae.) The K^+ electromagnetic analogue to the e-nucleus double differential cross section appearing in Eq. 20 is

$$
\frac{d^2\sigma}{d\omega d\Omega} = \frac{4\alpha^2}{(q^2)^2} \frac{p_f}{p_i} m^2 \left\{ \left(\frac{\epsilon_f + \epsilon_i}{2m} \right)^2 \left[\left(\frac{Q^2}{\mathbf{q}^2} \right)^2 W_{EM}^{00} + \frac{Q^2}{\mathbf{q}^2} W_{EM}^{11} \right] \right.
$$
$$
\left. - \left(1 + \frac{Q^2}{4m^2} \right) W_{EM}^{11} \right\} \tag{30}
$$

where now m is the K^+ mass.

Our next task is to generalize this treatment to handle *hadronic* interactions. For *electromagnetic* K^+ scattering, the t-matrix which leads to Eq. 26 is explicitly

$$T_{fi} = \frac{1}{V} \frac{1}{\sqrt{4\epsilon_f \epsilon_i}} \frac{-e^2}{q^2} p_\mu J_{fi}^\mu(\mathbf{q}). \tag{31}$$

where V is the box volume arising from box normalizing the free K^+ wavefunctions and where the electromagnetic transition current J^μ_{fi} is defined in Eq. 9. We next write

$$\frac{-e^2}{q^2} \, p_\mu \, J^\mu_{fi}(\mathbf{q}) \to \mathcal{F}'_{EM} \, \frac{p_\mu}{m} \, J^\mu_{fi}(EM), \quad \mathcal{F}'_{EM} \equiv \frac{-me^2}{q^2}. \tag{32}$$

Clearly, the dynamics specific to electromagnetic scattering appear only in the quantity $\mathcal{F}'_{EM}$; the remaining factors are of a form appropriate to a general 4-vector current-current interaction. We propose that for K^+ *hadronic* scattering, we should let

$$\mathcal{F}'_{EM} \, \frac{p_\mu}{m} \, J^\mu_{fi}(EM) \to \mathcal{F}'_S \, J^s_{fi} + \mathcal{F}'_V \, \frac{p_\mu}{m} \, J^\mu_{fi} \tag{33}$$

where now a scalar interaction appears in addition to the vector term. In this expression, $\mathcal{F}'_S$ and $\mathcal{F}'_V$ are complex numbers related to the K^+N elastic scattering amplitude in a manner to be established below and where the exact definitions of J^s_{fi} and J^μ_{fi} will be given shortly. It is plausible that an interaction of this form – while, as will be discussed below, not unique – is sufficiently general since we know that an on-shell spin 0-spin 1/2 elastic scattering amplitude can be completely specified at a given kinematic point (including an irrelevant overall phase) by two complex numbers. It is now convenient to introduce the notation

$$\mathcal{F}'_S \, J^s_{fi} + \mathcal{F}'_V \, \frac{p_\mu}{m} \, J^\mu_{fi} \to f'_a \, J^a_{fi}(\mathbf{q}) \tag{34}$$

where

$$f'_a \equiv \begin{cases} \mathcal{F}'_S & \text{for } a = s \\ \mathcal{F}'_V \, \frac{p_\mu}{m} & \text{for } a = \mu \end{cases} \tag{35}$$

and

$$J^a_{fi}(\mathbf{q}) = \int d^3y \, e^{+i\mathbf{q}\cdot\mathbf{y}} \ <f|\hat{\bar{\psi}}(\mathbf{y}) \, \Gamma^a \, \hat{\psi}(\mathbf{y})|i> \tag{36}$$

with

$$\Gamma^a \equiv \begin{cases} \mathbf{1} & \text{for } a = s \\ \gamma^\mu & \text{for } a = \mu \end{cases}. \tag{37}$$

With these definitions, it is straightforward to show that the *hadronic* K^+ cross section analogous to the electron and K^+ electromagnetic cross sections of Eqs. 1 and 26, respectively, is

$$d\sigma|_{had} = \frac{1}{v_{rel}} \, \frac{1}{4\pi^2} \, L_{ab} \, W^{ab} \, d^3p_f \tag{38}$$

where the K^+ hadronic tensor L_{ab} is defined as

$$L_{ab} \equiv \frac{f'^*_a f'_b}{4\epsilon_f \epsilon_i} \tag{39}$$

and the hadronic response is defined via (compare with Eqs. 4 through 6)

$$W^{ab} = -\frac{1}{\pi} \, \text{Im} \, \Pi^{ab}(\mathbf{q}, \mathbf{q}; \omega)$$

$$\Pi^{ab}(\mathbf{q}, \mathbf{q}'; \omega) = \int d^3y \; e^{-i\mathbf{q}\cdot\mathbf{y}} \int d^3y' \; e^{+i\mathbf{q}'\cdot\mathbf{y}'} \; \Pi^{ab}(\mathbf{y}, \mathbf{y}'; \omega) \tag{40}$$

where $\Pi^{ab}(\mathbf{y}, \mathbf{y}' : \omega)$ is specified by

$$\Pi^{ab}(y, y') = \frac{1}{i} < i|T[\hat{\Gamma}^a(y)\hat{\Gamma}^b(y')]|i >$$

$$= \int \frac{d\omega}{2\pi} \; e^{-i\omega(y^0 - y^{0'})} \; \Pi^{ab}(\mathbf{y}, \mathbf{y}'; \omega) \tag{41}$$

and $\hat{\Gamma}^a(y) = \bar{\hat{\psi}}(y)\Gamma^a\hat{\psi}(y)$.

We now specifically consider K^+N scattering. In Eq. 13 for electron scattering and Eq. 28 for K^+N electromagnetic scattering, we presented expressions for the differential cross sections in the initial nucleon rest frame. It is straight forward to derive a similar expression for the K^+N *hadronic* cross section. A slight generalization yields this cross section in a reference frame in which the K^+N relative motion is colinear but otherwise arbitrary. It will be convenient to have a formula for the K^+N *hadronic* cross section *in the center-of-momentum frame*, namely

$$\frac{d\bar{\sigma}}{d\Omega}\left(K^+N\right)\bigg|_{cm} = \frac{1}{2} \sum_{S_f S_i} \left| f_a \; \bar{u}(P_f S_f)\Gamma^a u(P_i S_i) \right|^2 \tag{42}$$

where

$$f_a \equiv \frac{1}{4\pi} \frac{E}{\epsilon + E} \; f_a'. \tag{43}$$

and where ϵ and E are the K^+ and N energies, respectively, in the center-of-momentum frame. It is straightforward to show

$$f_a \; \bar{u}(P_f S_f)\Gamma^a u(P_i S_i) = \bar{u}(P_f S_f)\left[\mathcal{F}_S + \mathcal{F}_V \frac{\not{p}}{m}\right]u(P_i S_i)$$

$$= \chi^\dagger(S_f) \left[F(q) + i\sigma_n G(q)\right] \chi(S_i) \tag{44}$$

where

$$\mathcal{F}_S = \frac{1}{4\pi} \frac{E}{\epsilon + E} \; \mathcal{F}_S', \quad \mathcal{F}_V = \frac{1}{4\pi} \frac{E}{\epsilon + E} \; \mathcal{F}_V' \tag{45}$$

and $\sigma_n \equiv \sigma \cdot \hat{n}$, $\hat{n} \equiv (\mathbf{p}_i \times \mathbf{p}_f)/|\mathbf{p}_i \times \mathbf{p}_f|$ as well as

$$F(q) = \frac{E+M}{2E}\left[\mathcal{F}_S\left(1 - \frac{E-M}{E+M}\cos\theta\right) + \frac{\epsilon}{m}\mathcal{F}_V\left(1 + \frac{E-M}{E+M}\cos\theta\right)\right]$$

$$+ \frac{E^2 - M^2}{2mE}\mathcal{F}_V\left(1 + \cos\theta\right) \tag{46}$$

and

8

$$G(q) = \left\{ \frac{E-M}{2E} \left[\mathcal{F}_S - \frac{\epsilon}{m} \mathcal{F}_V \right] - \frac{E^2 - M^2}{2mE} \mathcal{F}_V \right\} \sin\theta. \tag{47}$$

We recognize $F(q)$ and $G(q)$ as the Wolfenstein amplitudes for K^+-nucleon scattering and take them from Arndt's SP88 [13] K^+-proton and K^+-neutron phase shift solutions. The above relations may readily be inverted to find $\mathcal{F}_S$ and $\mathcal{F}_V$ or, equivalently, $\mathcal{F}'_S$ and $\mathcal{F}'_V$.

We finally investigate K^+-nucleus scattering. In analogy with Eq. 19 for e-nucleus scattering, the K^+-nucleus cross section in the nuclear rest frame is

$$\left. \frac{d^2\sigma}{d\omega d\Omega} \right|_{had} = \frac{1}{4\pi^2} \frac{\epsilon_i p_f \epsilon_f}{p_i} L_{ab} W^{ab}. \tag{48}$$

Using $q_\mu W^{\mu\nu} = q_\nu W^{\mu\nu} = q_\mu W^{\mu s} = 0$ which follows from the assumption that the baryon current is conserved and also using $W^{\mu s} = W^{s\mu}$, we can evaluate $L_{ab} W^{ab}$ to obtain – in analogy with Eq. 20 for e-nucleus scattering and Eq. 30 for K^+-nucleus electromagnetic scattering – the following K^+-nucleus hadronic cross section:

$$\begin{aligned}
\left. \frac{d^2\bar\sigma}{d\omega d\Omega} \right|_{had} = \frac{1}{16\pi^2} \frac{p_f}{p_i} \Bigg[\ & |\mathcal{F}'_S|^2 W^{ss} \\
& + |\mathcal{F}'_V|^2 \bigg\{ \left(\frac{\epsilon_f + \epsilon_i}{2m} \right)^2 \left[\left(\frac{Q^2}{\mathbf{q}^2} \right)^2 W^{00} + \frac{Q^2}{\mathbf{q}^2} W^{11} \right] \\
& \qquad\qquad - \left(1 + \frac{Q^2}{4m^2} \right) W^{11} \bigg\} \\
& + 2\mathrm{Re}(\mathcal{F}'_S \mathcal{F}'^*_V) \left(\frac{\epsilon_f + \epsilon_i}{2m} \right) \frac{Q^2}{\mathbf{q}^2} W^{0s} \Bigg].
\end{aligned} \tag{49}$$

This is the main result of Section III. We note that two new responses – namely W^{ss} and W^{0s} – which were not present for the electromagnetic processes enter in the hadronic cross section.

We finally observe that, for a single nucleon, the hadronic responses W^{00} and W^{11} are given by the corresponding single nucleon electromagnetic responses of Eqs. 24 and 25 in the limit that $F_1 \to 1$ and $F_2 \to 0$ or, equivalently, $G_E, G_M \to 1$. Furthermore, it is easy to show that, in the initial nucleon rest frame, $W^{ss} = W^{s0} = W^{00} = (1+\tau)/(1+2\tau)$ for a single nucleon.

IV. ON-SHELL AMBIGUITIES FOR PROJECTILE-NUCLEON INTERACTIONS

The expression for the electromagnetic current of a *free* nucleon (Eq. 9) contains the matrix element of the nucleon electromagnetic current operator, Γ^μ_{EM} (Eq. 7), evaluated between *free* nucleon Dirac spinors. Using the Gordon decomposition, we may write

$$\bar{u}(P_f, S_f) \, \Gamma^\mu_{EM} \, u(P_i, P_f) = \bar{u}(P_f, S_f) \, \Gamma^\mu_{EM}(\xi) \, u(P_i, P_f) \tag{50}$$

where

$$\Gamma^\mu_{EM}(\xi) \equiv F_S(\xi) \frac{(P_f + P_i)^\mu}{2M} + F_V(\xi) \gamma^\mu + i F_T(\xi) \frac{\sigma^{\mu\nu}(P_f - P_i)_\nu}{2M} \tag{51}$$

9

with

$$F_S(\xi) \equiv -\xi F_2, \qquad F_V(\xi) \equiv F_1 + \xi F_2, \qquad F_T(\xi) \equiv (1 - \xi)F_2 \qquad (52)$$

and where ξ is *arbitrary*. In reference to the *Dirac* character of the operators in the three terms (as opposed to their *Lorentz* character which is of course vectorial on all three cases), we have identified the first through third terms as "scalar", "vector" and "tensor", respectively. We may then transform to three distinct on-shell equivalent forms of Γ^μ_{EM} each containing only two terms according to

$$
\begin{aligned}
\xi = 0 &\quad\leftrightarrow\quad \text{VT} \\
\xi = 1 &\quad\leftrightarrow\quad \text{VS} \\
\xi = -F_1/F_2 &\quad\leftrightarrow\quad \text{ST}
\end{aligned}
$$

where, *e.g.*, "VT" means that only vector and tensor terms are present. (Note that, in evaluating the free nucleon electromagnetic tensor, $\ell^{\mu\nu}(N)$ of Eq. 11, it is most convenient to employ the VS (or $\xi = 1$) form of $\Gamma^\mu_{EM}(\xi)$.)

The impulse approximation used in Section II to evaluate the *nuclear* (e, e') cross section does not in and of itself prescribe which representation of $\Gamma^\mu_{EM}(\xi)$ to use. This well-known ambiguity is problematic since as soon as the nucleon wave functions are modified by the nuclear medium, the various forms of $\Gamma^\mu_{EM}(\xi)$ are no longer equivalent. Put another way, if we define the generalized electromagnetic response, $W^{\mu\nu}_{EM}(\xi)$, just as in Eqs. 4 through 6, except that $\Gamma^\mu_{EM}(\xi)$ is employed in Eq. 6, we find that $W^{\mu\nu}_{EM}(\xi)$ is not generally independent of ξ. This represents an important qualification of the oft-repeated statement that the nuclear electromagnetic interaction is well-understood. (There are, of course, any number of other effects which can modify the in-medium electromagnetic interaction; we are at present restricting our attention to the ambiguities inherent in the *impulse approximation*.) It is worth noting that the ξ-dependence of electromagnetic observables is especially strong in the relativistic model of nuclear structure we will employ and which is outlined in Section V. A definitive resolution of the ξ ambiguity awaits a dynamical description of nucleon structure and how it is affected by the nuclear environment. We do not, of course, propose to solve that problem here. Indeed, we simply adopt the VT or $\xi = 0$ form of $\Gamma^\mu_{EM}(\xi)$ according to "conventional wisdom" [14].

Since the treatment of K^+-nucleus scattering presented in Section III is also based on the impulse approximation applied to the underlying K^+N interaction, it is plagued by its own on-shell ambiguities. In the expression for the center-of-momentum frame K^+N cross section (Eq. 42), we find the free nucleon matrix element

$$
\begin{aligned}
&f_a \ \bar{u}(P_f S_f) \ \Gamma^a \ u(P_i S_i) \\
&= \bar{u}(P_f S_f)\Big[\mathcal{F}_S \ \mathbf{1} + \mathcal{F}_V \frac{\not{p}}{m}\Big] u(P_i S_i) \\
&= \bar{u}(P_f S_f)\Big\{\mathcal{F}_S(\xi) \ \mathbf{1} + \frac{p_\mu}{m}\Big[\mathcal{F}_V(\xi)\gamma^\mu + i\mathcal{F}_T(\xi)\frac{\sigma^{\mu\nu}(P_f - P_i)_\nu}{2M}\Big]\Big\} u(P_i S_i) \qquad (53)
\end{aligned}
$$

where

$$\mathcal{F}_S(\xi) \equiv \mathcal{F}_S + \xi \mathcal{F}_V \frac{p \cdot P}{mM}\,, \qquad \mathcal{F}_V(\xi) \equiv (1 - \xi)\mathcal{F}_V\,, \qquad \mathcal{F}_T(\xi) \equiv \xi\mathcal{F}_V \qquad (54)$$

and ξ is again arbitrary. We have once more identified Dirac scalar, vector and tensor terms and may also define scalar, vector and tensor forms of the interaction according to

$$\xi = 0 \qquad \leftrightarrow \qquad \text{VT}$$
$$\xi = 1 \qquad \leftrightarrow \qquad \text{VS}$$
$$\xi = -\mathcal{F}_S / \left(\mathcal{F}_V \frac{p \cdot P}{mM} \right) \qquad \leftrightarrow \qquad \text{ST}.$$

(We note that, by choosing the VT form of the $K^+ N$ interaction, K^+ hadronic scattering becomes – in plane wave Born approximation – *formally* identical to the (fictitious) K^+ electromagnetic process discussed in the beginning of Section III.) As will be discussed in detail below, K^+-nucleus cross sections show some sensitivity to the form of the $K^+ N$ interaction. Since there is no "conventional wisdom" to guide our choice as there was for electron scattering, we must appeal to a dynamical model of $K^+ N$ scattering for help in resolving the on-shell ambiguity.

We turn specifically to the meson exchange model of $K^+ N$ scattering developed by the Bonn group [15] along the lines of their model of the NN interaction. This model has as its input parameters meson masses, K^+-meson and N-meson coupling constants and form factors. Certain of the interactions implied by these couplings are iterated to all orders and the resulting phase shifts are in good agreement with those determined by experiment. For our purposes, we focus on the $K^+ N$ interactions mediated by the exchange of ρ, ω and (fictitious) σ mesons. To proceed, we identify the T=0 (isoscalar) and T=1 (isovector) combinations of the $K^+ N$ elastic scattering amplitude. In terms of, *e.g.*, the Wolfenstein amplitudes of Eq. 44, we define

$$F_{T=0} \equiv \frac{1}{2}(F_p + F_n) , \qquad F_{T=1} \equiv \frac{1}{2}(F_p - F_n) \qquad (55)$$

where F_p (F_n) is the K^+-proton (K^+-neutron) amplitude. The isoscalar and isovector pieces of $\mathcal{F}'_S$ and $\mathcal{F}'_V$ then follow as described at the end of Section III. For $N = Z$ targets, the K^+-nucleus cross section is simply the sum of T=0 and T=1 contributions given by Eq. 49 with different $\mathcal{F}'$'s and W^{ab} 's for each isospin.

In Born approximation, ρ exchange contributes to the isovector amplitudes while ω and σ exchange contribute to the isoscalar amplitudes. Since the ρN coupling has a vector-tensor Dirac character (with the tensor component dominant), the *Born* isovector amplitude generated by ρ exchange has a VT (or, referring to Eq. 52, a $\xi = -\mathcal{F}_S / \left(\mathcal{F}_V \frac{p \cdot P}{mM} \right)$) form. Numerically, the ρ exchange Born amplitude predicted by the Bonn model at the kinematic point appropriate to the $|\mathbf{q}| = 500$ MeV/c K^+-nucleus data, namely $p_i = 705$ MeV/c and $\theta_{lab} = 43$ degrees [9,10], is qualitatively consistent with the empirical amplitude [13] we employ. (Specifically, dominance of $\mathcal{F}_T$ over $\mathcal{F}_V$ is observed.) Similarly, since the ωN coupling is assumed to be purely vector, the Born isoscalar amplitude due to σ and ω exchange has a VS (or $\xi = 0$) form. Again, the Born amplitudes from the Bonn model are qualitatively consistent with the relevant empirical results. Specifically, it is observed that $\mathcal{F}_S$ and $\mathcal{F}_V$ are of opposite signs (the scalar interaction is attractive) and are nearly equal in magnitude.

The arguments presented above are clearly only suggestive. While we have argued that the form for the $K^+ N$ interaction employing the VS representation for the isoscalar amplitudes and the VT representation for the isovector amplitudes is physically most plausible,

we will also show in the analysis to follow calculations which utilize the VS representation for both the isoscalar and isovector amplitudes.

V. NUCLEAR STRUCTURE

In this section we describe our nuclear structure model. Throughout this paper we assume the impulse approximation to be valid. Hence, apart from the ambiguities addressed in the previous section, the in-medium e^-N and K^+N couplings are entirely determined from on-shell data. Moreover, we assume that both sets of couplings are small so that distortions and multi-step processes (*e.g.*, multi-photon exchanges in the case of (e,e')) may be ignored. In this framework, all relevant nuclear structure information is contained in the responses of the nuclear target introduced in Sections II and III to be discussed further in this section.

The response of the nuclear target will be calculated in a relativistic random-phase-approximation to the Walecka model. In the Walecka model nucleons interact via the exchange of isoscalar scalar (σ) and vector (ω) fields. The dynamics of the system is, thus, described in terms of the following Lagrangian density

$$\mathcal{L} = \bar{\psi}(i\not{\partial} - M)\psi + \frac{1}{2}(\partial_\mu\phi\partial^\mu\phi - m_{\mathrm{s}}^2\phi^2) - \frac{1}{4}F_{\mu\nu}F^{\mu\nu}$$
$$+ g_{\mathrm{s}}\bar{\psi}\psi\phi - g_{\mathrm{v}}\bar{\psi}\gamma^\mu\psi V_\mu + \delta\mathcal{L} , \tag{56}$$

where $g_{\mathrm{s}}(g_{\mathrm{v}})$ is the scalar(vector) coupling constant, M, m_s, and m_v are the nucleon, σ-meson, and ω-meson masses, respectively, and ψ, ϕ, and V^μ are the corresponding field operators. The term $\delta\mathcal{L}$ contains renormalization counterterms and the antisymmetric field-strength tensor, $F_{\mu\nu}$, has been defined by

$$F_{\mu\nu} \equiv \partial_\mu V_\nu - \partial_\nu V_\mu . \tag{57}$$

The nuclear ground state will be obtained in a relativistic mean field approximation to the Walecka model. In this case, the meson-field operators are replaced by their ground-state expectation values. This approximation yields a set of Dirac single-particle states that are determined self-consistently from the equations of motion.

The one-body response of the nuclear ground state to an external probe is fully contained in the polarization tensor. The polarization tensor is a fundamental many-body operator that can be systematically computed using well-known many-body techniques (e.g., Feynman diagrams). To illustrate these techniques we concentrate on the vector polarization, for simplicity. This is defined as the ground-state expectation value of a time-ordered product of nuclear (vector) currents

$$\Pi^{\mu\nu}(x,y) = \frac{1}{i}\langle i|T\Big[J^\mu(x)J^\nu(y)\Big]|i\rangle . \tag{58}$$

In a mean-field approximation to the ground state the polarization insertion can be written, exclusively, in terms of the single-nucleon propagator $G(x,y)$

$$\Pi^{\mu\nu}(x,y) = \frac{1}{i}\mathrm{Tr}\left[\gamma^\mu G(x,y)\gamma^\nu G(y,x)\right] . \tag{59}$$

The nucleon propagator contains information about the interaction of the nucleon with the average mean field provided by the nuclear medium. Note that even if the interactions are ignored, such as in a Fermi-gas description, the propagator would still be different than its free-space value because of the existence of a filled Fermi sea. This fact suggests the following decomposition of the nucleon propagator

$$G(x, y) = \int_{-\infty}^{\infty} \frac{d\omega}{2\pi} e^{-i\omega(x^0 - y^0)} G(\mathbf{x}, \mathbf{y}; \omega) , \tag{60}$$

$$G(\mathbf{x}, \mathbf{y}; \omega) = G_F(\mathbf{x}, \mathbf{y}; \omega) + G_D(\mathbf{x}, \mathbf{y}; \omega) . \tag{61}$$

The Feynman part of the propagator, G_F, has the same analytic structure as the free propagator, namely, antiparticle poles above the real axis, particle poles below the real axis, and residues proportional to the single-particle wave functions

$$G_F(\mathbf{x}, \mathbf{y}; \omega) = \sum_\alpha \left[\frac{U_\alpha(\mathbf{x}) \overline{U}_\alpha(\mathbf{y})}{\omega - E_\alpha^{(+)} + i\eta} + \frac{V_\alpha(\mathbf{x}) \overline{V}_\alpha(\mathbf{y})}{\omega + E_\alpha^{(-)} - i\eta} \right] . \tag{62}$$

The density-dependent part of the propagator, G_D, corrects G_F for the presence of a filled Fermi surface. Formally, one effects this correction by shifting the position of the pole of every occupied state from below to above the real axis

$$G_D(\mathbf{x}, \mathbf{y}; \omega) = \sum_{\alpha < \mathrm{F}} U_\alpha(\mathbf{x}) \overline{U}_\alpha(\mathbf{y}) \left[\frac{1}{\omega - E_\alpha^{(+)} - i\eta} - \frac{1}{\omega - E_\alpha^{(+)} + i\eta} \right] \tag{63}$$

$$= 2\pi i \sum_{\alpha < \mathrm{F}} \delta\left(\omega - E_\alpha^{(+)}\right) U_\alpha(\mathbf{x}) \overline{U}_\alpha(\mathbf{y}) . \tag{64}$$

The decomposition of the nucleon propagator into Feynman and density-dependent contributions suggests an equivalent decomposition for the polarization insertion

$$\Pi^{\mu\nu}(x, y) = \int_{-\infty}^{\infty} \frac{d\omega}{2\pi} e^{-i\omega(x^0 - y^0)} \Pi^{\mu\nu}(\mathbf{x}, \mathbf{y}; \omega) , \tag{65}$$

$$\Pi^{\mu\nu}(\mathbf{x}, \mathbf{y}; \omega) = \Pi_F^{\mu\nu}(\mathbf{x}, \mathbf{y}; \omega) + \Pi_D^{\mu\nu}(\mathbf{x}, \mathbf{y}; \omega) . \tag{66}$$

The Feynman part of the polarization, or vacuum polarization, Π_F, describes the excitation of nucleon-antinucleon $(N\overline{N})$ pairs

$$\Pi_F^{\mu\nu}(\mathbf{x}, \mathbf{y}; \omega) = \frac{1}{i} \int_{-\infty}^{\infty} \frac{d\omega'}{2\pi} \mathrm{Tr}\left[\gamma^\mu G_F(\mathbf{x}, \mathbf{y}; \omega + \omega') \gamma^\nu G_F(\mathbf{y}, \mathbf{x}; \omega') \right] . \tag{67}$$

Note that this contribution diverges and must be renormalized. A lowest order calculation of the response, however, requires of only the imaginary part of the polarization insertion. In infinite nuclear matter, the threshold for pair production is at $q_\mu^2 = 4M^{*2} > 0$ (M^* is the effective nucleon mass in the medium). This timelike threshold lies far away from the spacelike region accessible in electron and kaon scattering. Thus, a lowest-order description of the process is not sensitive to vacuum polarization. However, $N\overline{N}$ excitations can be virtually produced. Hence, in a more sophisticated treatment of the response (e.g., RPA) the effective coupling of the nucleon to the probe can be modified by vacuum polarization. Indeed, it has been suggested that virtual $N\overline{N}$ pairs play an important role in the quenching of the Coulomb sum [17].

The density-dependent part of the polarization, Π_D, is finite and can be organized in terms of three distinct contributions

$$\Pi_D^{\mu\nu}(\mathbf{x}, \mathbf{y}; \omega) = \Pi_{FD}^{\mu\nu}(\mathbf{x}, \mathbf{y}; \omega) + \Pi_{DF}^{\mu\nu}(\mathbf{x}, \mathbf{y}; \omega) + \Pi_{DD}^{\mu\nu}(\mathbf{x}, \mathbf{y}; \omega) , \tag{68}$$

with each one of them of at least linear in G_D

$$\Pi_{FD}^{\mu\nu}(\mathbf{x}, \mathbf{y}; \omega) = \sum_{\alpha<F} \overline{U}_\alpha(\mathbf{x}) \gamma^\mu G_F\Big(\mathbf{x}, \mathbf{y}; E_\alpha^{(+)} + \omega\Big) \gamma^\nu U_\alpha(\mathbf{y}) , \tag{69}$$

$$\Pi_{DF}^{\mu\nu}(\mathbf{x}, \mathbf{y}; \omega) = \sum_{\alpha<F} \overline{U}_\alpha(\mathbf{y}) \gamma^\nu G_F\Big(\mathbf{y}, \mathbf{x}; E_\alpha^{(+)} - \omega\Big) \gamma^\mu U_\alpha(\mathbf{x}) , \tag{70}$$

$$\Pi_{DD}^{\mu\nu}(\mathbf{x}, \mathbf{y}; \omega) = 2\pi i \sum_{\alpha<F} \sum_{\alpha'<F} \Big[\overline{U}_\alpha(\mathbf{x})\gamma^\mu U_{\alpha'}(\mathbf{x})\Big]\Big[\overline{U}_{\alpha'}(\mathbf{y})\gamma^\nu U_\alpha(\mathbf{y})\Big]\delta\Big(\omega + E_\alpha^{(+)} - E_{\alpha'}^{(+)}\Big) . \tag{71}$$

The density-dependent part of the polarization describes the traditional excitation of particle-hole pairs. A spectral decomposition of the Feynman propagator, for Π_{FD}, is useful when discussing the spectral content of the polarization (the Π_{DF} term, with the opposite time ordering, contains the same physical information as Π_{FD})

$$\Pi_{FD}^{\mu\nu}(\mathbf{x}, \mathbf{y}; \omega) = \sum_{\alpha<F,\beta} \left[\frac{\overline{U}_\alpha(\mathbf{x})\gamma^\mu U_\beta(\mathbf{x})\overline{U}_\beta(\mathbf{y})\gamma^\nu U_\alpha(\mathbf{y})}{\omega - \Big(E_\beta^+ - E_\alpha^+\Big) + i\eta} + \frac{\overline{U}_\alpha(\mathbf{x})\gamma^\mu V_\beta(\mathbf{x})\overline{V}_\beta(\mathbf{y})\gamma^\nu U_\alpha(\mathbf{y})}{\omega + \Big(E_\beta^- + E_\alpha^+\Big) - i\eta} \right] . \tag{72}$$

The first term in the sum represents the formation of a particle-hole pair after the system has absorbed (e.g., a photon carrying) energy ω. Note, however, that some of these particle-hole transitions should be Pauli-blocked since the Feynman part of the propagator includes an unrestricted (β) sum over all single-particle states. The role of Π_{DD} in the present formalism is, precisely, to enforce the Pauli principle. Note that since the Feynman part of the propagator will be evaluated nonspectrally, these Pauli-forbidden transition can not be simply removed by hand.

The density-dependent part of the polarization contains, in addition to particle-hole pairs, a contribution that has no nonrelativistic counterpart. This contribution is contained in the second term of the sum and represents the Pauli blocking of $N\overline{N}$ excitations. Recall that the Feynman part of the polarization insertion represents the unconstrained excitation of $N\overline{N}$ pairs. At finite density, however, some of these excitations should be Pauli-blocked.

It is important to note that the inclusion of antinucleon degrees of freedom is not an unnecessary complication. If one is satisfied with computing the lowest order, or uncorrelated, nuclear response, then a "nucleons-only" approximation is certainly justified. If, however, one wishes to examine the role of correlations by means of an RPA response, then one is forced to include antinucleon degrees of freedom in order to satisfy fundamental physical principles such as gauge invariance.

Traditionally, relativistic calculations of the nuclear response have been carried out using two mean-field approximations to the Walecka model. In the mean-field theory (MFT) the Feynman contribution to the single-particle propagator is neglected from the calculation of the nucleon self-energy. In contrast, one incorporates the effect from the (full) Dirac sea in the relativistic Hartree approximation (RHA). For a mean-field ground state obtained in

the MFT approximation, it has been shown that the consistent linear response of the mean-field ground state is obtained by neglecting the Feynman part of the polarization insertion. This consistency is reflected, for example, in the proper treatment of spurious excitations associated with an overall translation of the center of mass. Notice, however, that in the MFT approximation one retains the Pauli blocking of an $(N\bar{N})$ excitation that has not been included from the outset. It has recently been shown that this approximation leads to severe inconsistencies in the description of the effective ω-meson mass in the nuclear medium [19]. Thus, in this work we favor an RHA treatment of the scattering process in which vacuum loops are included in both the description of the ground state as well as in the linear response of the system.

We start with a discussion of the density-dependent contribution to the polarization. This contribution is finite and can be evaluated exactly in the finite system. According to Eq. (69) we must compute — self-consistently — all occupied single-particle states and the Feynman part of the propagator. The calculation proceeds by, first, calculating a set of occupied single-particle states satisfying the following Dirac equation

$$\left[E_\alpha^{(+)}\gamma^0 + i\gamma\cdot\partial - M - \Sigma_H(\mathbf{x})\right]U_\alpha(\mathbf{x}) = 0 \ . \tag{73}$$

A Hartree calculation of the mean-field ground state yields, in addition to the single-particle spectrum, the self-consistent (scalar and vector) mean-fields used to generate the spectrum

$$\Sigma_H(\mathbf{x}) = \Sigma_{\rm s}(\mathbf{x}) + \Sigma_{\rm v}(\mathbf{x})\gamma^0 \ . \tag{74}$$

Knowledge of the self-consistent mean fields now enables one to compute — nonspectrally — the Feynman part of the nucleon propagator by solving the equation

$$\left[\omega\gamma^0 + i\gamma\cdot\partial - M - \Sigma_H(\mathbf{x})\right]G_F(\mathbf{x},\mathbf{y};\omega) = \delta(\mathbf{x}-\mathbf{y}) \ , \tag{75}$$

with the appropriate boundary conditions.

The evaluation of the polarization insertion, although still highly nontrivial, gets simplified for the case of a spherically symmetric ground state. In this case, one can classify the single-particle states according to a generalized angular momentum κ

$$U_{E\kappa m}(\mathbf{x}) = \frac{1}{x}\left(\begin{array}{c} g_{E\kappa}(x)\mathcal{Y}_{\kappa m}(\hat{\mathbf{x}}) \\ if_{E\kappa}(x)\mathcal{Y}_{\bar{\kappa}m}(\hat{\mathbf{x}}) \end{array}\right) \ , \tag{76}$$

where $\bar{\kappa} \equiv -\kappa$ and we have introduced the spin-spherical harmonics defined by

$$\mathcal{Y}_{\kappa m}(\hat{\mathbf{x}}) = \langle\hat{\mathbf{x}}|l\frac{1}{2}jm\rangle \ , \quad \kappa = \begin{cases} l, & \text{if } l = j + 1/2 \ ; \\ -l-1, & \text{if } l = j - 1/2 \ . \end{cases} \tag{77}$$

The Feynman part of the propagator can be, similarly, written as a sum over partial waves

$$G_F(\mathbf{x},\mathbf{y};\omega) = \frac{1}{xy}\sum_{\kappa m}\left(\begin{array}{cc} g_{11}^\kappa(x,y;\omega)\mathcal{Y}_{\kappa m}(\mathbf{x})\mathcal{Y}_{\kappa m}^\dagger(\mathbf{y}) & -ig_{12}^\kappa(x,y;\omega)\mathcal{Y}_{\kappa m}(\mathbf{x})\mathcal{Y}_{\bar{\kappa}m}^\dagger(\mathbf{y}) \\ +ig_{21}^\kappa(x,y;\omega)\mathcal{Y}_{\bar{\kappa}m}(\mathbf{x})\mathcal{Y}_{\kappa m}^\dagger(\mathbf{y}) & g_{22}^\kappa(x,y;\omega)\mathcal{Y}_{\bar{\kappa}m}(\mathbf{x})\mathcal{Y}_{\bar{\kappa}m}^\dagger(\mathbf{y}) \end{array}\right) \ . \tag{78}$$

Once the bound-state orbitals and the Feynman propagator have been determined, the evaluation of the polarization tensor in momentum space

$$\Pi^{\mu\nu}(\mathbf{q}, \mathbf{q}'; \omega) = \int d^3x \; e^{-i\mathbf{q}\cdot\mathbf{x}} \int d^3y \; e^{i\mathbf{q}'\cdot\mathbf{y}} \Pi^{\mu\nu}(\mathbf{x}, \mathbf{y}; \omega) , \tag{79}$$

becomes straightforward. The angular integrals are done analytically leaving two radial integrals to be performed numerically. We stress that the procedure outlined above enables one to calculate the density-dependent part of the polarization exactly in the finite system.

The Feynman part of the polarization, however, must be calculated in a local-density approximation. To our knowledge, the renormalization of the divergent integrals has never been carried out in the finite system. Thus, in the present work we adopt the following form for the Feynman contribution to the response

$$\Pi_F^{\mu\nu}(\mathbf{q}, \mathbf{q}'; \omega) = \int d^3r \; e^{-i(\mathbf{q}-\mathbf{q}')\cdot\mathbf{r}} \Pi_F^{\mu\nu}\left(\bar{\mathbf{q}}, \omega; M^*(r)\right) , \tag{80}$$

where $\Pi_F^{\mu\nu}\left(\bar{\mathbf{q}}, \omega; M^*(r)\right)$ is the renormalized vacuum polarization calculated in nuclear matter at an average momentum $\bar{\mathbf{q}} = (\mathbf{q} + \mathbf{q}')/2$, and at a local value of the effective nucleon mass

$$M^*(r) = M + \Sigma_{\rm s}(r) . \tag{81}$$

The nuclear response will be calculated in a variety of models and approximations. The most sophisticated calculation that we will present involves calculating the nuclear response in a relativistic random phase approximation (RPA) to the Walecka model. In RPA one incorporates many-body correlations through an infinite summation of the lowest order (or uncorrelated) polarization. Due to scalar-vector mixing the RPA equations form a set of 5×5 coupled integral equations

$$\Pi_{\rm RPA}^{ab}(\mathbf{q}, \mathbf{q}'; \omega) = \Pi^{ab}(\mathbf{q}, \mathbf{q}'; \omega) + \int \frac{d^3k}{(2\pi)^3} \Pi^{ac}(\mathbf{q}, \mathbf{k}; \omega) V_{cd}(\mathbf{k}; \omega) \Pi_{\rm RPA}^{db}(\mathbf{k}, \mathbf{q}'; \omega) , \tag{82}$$

where we have introduced latin indices $a \equiv (s, \mu)$ that run over scalar and vector Lorentz structures, and a residual interaction V_{ab} given by

$$V_{ab}(\mathbf{q}; \omega) \equiv V_{ab}(q) = \begin{pmatrix} g_{\rm s}^2 \Delta(q) & 0 \\ 0 & g_{\rm v}^2 D_{\mu\nu}(q) \end{pmatrix} . \tag{83}$$

Note that the free vector and scalar propagators have been defined, respectively, by

$$D_{\mu\nu}(q) = \left(-g_{\mu\nu} + q_\mu q_\nu/m_{\rm v}^2\right) D(q) , \tag{84}$$

$$D(q) = \frac{1}{q_\mu^2 - m_{\rm v}^2} , \tag{85}$$

$$\Delta(q) = \frac{1}{q_\mu^2 - m_{\rm s}^2} . \tag{86}$$

The RPA equations are solved — for every spin and parity J^π — by, first, performing the radial (k)-integral using a Gauss quadrature scheme and then solving the resulting matrix equation using standard matrix-inversion techniques.

We conclude this section with a brief discussion of the response of infinite nuclear matter. Due to the translational-invariant character of nuclear matter the previous discussion

simplifies considerably. In a mean-field approximation to the Walecka model the meson-field operators are replaced by their classical ground-state expectation values which are constants in nuclear matter

$$\phi \rightarrow \langle\phi\rangle \equiv \phi_0 \, , \tag{87}$$

$$V^\mu \rightarrow \langle V^\mu\rangle \equiv g^{\mu 0}V^0 \, . \tag{88}$$

The ground-state of the system is, thus, characterized by a filled Fermi (and Dirac) sea of nucleons with an effective mass M^* determined self-consistently from the equations of motion

$$M^* \equiv M - g_\mathrm{s}\phi_0 \, , \tag{89}$$

and effective nucleon and antinucleon energies which are shifted by the presence of a constant vector field

$$E_\mathbf{k}^{(\pm)} \equiv E_\mathbf{k}^* \pm g_\mathrm{v}V^0 \, , \tag{90}$$

$$E_\mathbf{k}^* \equiv \sqrt{\mathbf{k}^2 + M^{*2}} \, . \tag{91}$$

In particular, this implies that the nucleon propagator is, formally, indistinguishable from the free nucleon propagator. The Feynman and density-dependent propagators, which are the basic building blocks for the response, are thus given, respectively, by

$$G_F(k) = \left(\bar{\slashed{k}} + M^*\right)\left[\frac{1}{\bar{k}^2 - M^{*2} + i\eta}\right] \, , \tag{92}$$

$$G_D(k) = \left(\bar{\slashed{k}} + M^*\right)\left[\frac{i\pi}{E_\mathbf{k}^*}\delta\!\left(\bar{k}^0 - E_\mathbf{k}^*\right)\theta\!\left(k_\mathrm{F} - |\mathbf{k}|\right)\right] \, , \tag{93}$$

where k_F is the Fermi momentum and we have defined

$$\bar{k}^\mu \equiv (k^0 - g_\mathrm{v}V^0, \mathbf{k}) \, . \tag{94}$$

From the nucleon propagator it is simple to construct the lowest-order nuclear response

$$i\Pi^{\mu\nu}(q) = \int \frac{d^4k}{(2\pi)^4}\mathrm{Tr}\!\left[\gamma^\mu G(k+q)\gamma^\nu G(k)\right] \, . \tag{95}$$

As before, the polarization contains a divergent Feynman component that must be renormalized, and a finite density-dependent contribution that describes particle-hole excitations and the Pauli blocking of $N\overline{N}$ pairs. From this lowest order polarization one computes the correlated response by solving the RPA equation which becomes, in nuclear matter, a simple algebraic equation.

The only ingredients that remain to be specified are the effective number of nucleons and for nuclear-matter calculations the average density at which the scattering occurs. These quantities are determined from eikonal formulae that read:

$$A_\mathrm{eff} = \int d^3r \, e^{-\sigma t(b)}\rho(r) \, , \tag{96}$$

$$\rho_\mathrm{eff} = \frac{1}{A_\mathrm{eff}}\int d^3r \, e^{-\sigma t(b)}\rho^2(r) \equiv \frac{2k_\mathrm{F}^3}{3\pi^2} \, , \tag{97}$$

where σ is the elementary projectile-nucleon total cross section and $t(b)$ is the nuclear-thickness function defined by

$$t(b) = \int_{-\infty}^{\infty} dz \, \rho(r) \, . \tag{98}$$

From the effective density a self-consistent nucleon mass M^* is determined [16] which then serves as input for the calculation of the various nuclear responses per nucleon. These responses are subsequently scaled by the effective number of nucleons A_{eff} and then compared to experiment. In the case of e^--nucleus scattering we ignore the small electromagnetic distortions (i.e., assume $\sigma \equiv 0$) and compute for ^{40}Ca: $A_{\mathrm{eff}} = 40$, $k_{\mathrm{F}} = 1.13$ fm^{-1}, and $M^*/M = 0.81$. The equivalent expressions for K^+-nucleus scattering (where the isospin-averaged total cross section is $\sigma = 14.12$ mb) become: $A_{\mathrm{eff}} = 16.06$, $k_{\mathrm{F}} = 1.04$ fm^{-1}, and $M^*/M = 0.84$. (Note that we use *experimentally* determined [9,10] values of A_{eff} to normalize the K^+ quasielastic calculations to be presented below. The reason for the discrepancy between our eikonal estimates and the experimental value of $A_{\mathrm{eff}} \simeq 21$ is not understood at present.)

VI. RESULTS

We begin our comparison of e^- and K^+ quasielastic scattering by presenting calculations of the longitudinal (or Coulomb) and transverse (e, e') responses for ^{40}Ca at $|\mathbf{q}| = 500$ MeV/c in Figures 1 and 2, respectively. The data are from Reference [1]. All calculations are based on the relativistic Hartree approximation (RHA) to QHD as described in the previous section and thus include effects due to polarization of the nucleon sea at the one-loop level. We show both nuclear matter (NM) and finite nucleus (FN) calculations without (Har) and with (RPA) RPA correlations. Figure 1 clearly shows the dramatic quenching of the longitudinal response due to the RPA which results in reasonable agreement with experiment. As explained in, *e.g.*, Ref. [17], this quenching is most readily interpreted as a screening of the nucleon charge due to polarization of the nucleon sea. The magnitude of the quenching is comparable for NM and FN calculations but an acceptable description of the shape of the measured response evidently requires inclusion of finite nucleus effects. Figure 2 compares our calculations with the measured transverse response. Since, as for all calculations reported here, we have included isoscalar correlations only, the differences between Har and RPA results are small for this predominantly isovector response. Good agreement with experiment is found for the low-energy side of the quasielastic peak, especially for the finite nucleus calculations. The underestimation of transverse strength on the high-energy side of the peak, believed to be dominated by isobar formation and meson-exchange currents, is a common shortcoming of most "one-nucleon" models such as ours.

Comparable calculations are displayed with the K^+ data [9,10] in Figures 3 and 4 where we employ the VS and mixed VS (for T=0) and VT (for T=1) representations, respectively, for the K^+N t-matrix as discussed in Section IV. In Figure 3 the calculations are normalized using $A_{eff} = 21$ which is the mean value extracted from experiment [9,10]. The calculations appearing in Figure 4 use $A_{eff} = 24$ which is the experimental upper limit. The agreement between our most complete calculations, namely those labelled FN(RPA), and the data is excellent although the VS calculations reproduce the overall magnitude of the measured

cross sections slightly better than the mixed VS-VT results which slightly underestimate the measurements. We note that, while the simple mass M Fermi-gas result reproduces the observed *peak* K^+ quasielastic cross section of ≈ 0.24 mb/sr/MeV using the eikonal value of $A_{eff} = 16$, its accounting of the *shape* of the cross section is poor. In particular, the mass M Fermi-gas cross section peaks at $\omega \approx 85$ MeV and drops too rapidly at high ω, vanishing at $\omega \approx 210$ MeV. For this reason, the mass M Fermi-gas calculations must be considered inadequate regardless of normalization. Returning to the full calculations, we see that two differences relative to the (e, e') calculations are immediately apparent. First, NM and FN calculations are much more alike for K^+ than for (e, e'). Second and more striking is the fact that RPA effects are relatively small for the K^+ cross sections in contrast to the large quenching they generate for the (e, e') longitudinal response. This difference is even more surprising since the K^+ cross section is *dominated* by "longitudinal" contributions (*i.e.*, by terms in Eq. 49 not involving W^{11}) which are closely related to the (e, e') longitudinal response. We will show that this difference arises from a subtle interplay of kinematic and relativistic nuclear structure effects. In the course of this discussion, we will see that the lack of strong quenching in K^+ quasielastic scattering is quite remarkable since the additional "longitudinal" responses appearing in Eq. 49, namely W^{ss} and W^{0s}, are quenched *even more* than W^{00} to which the (e, e') longitudinal response is most closely related.

To understand the important physical contributions which determine the (e, e') longitudinal response and the K^+ quasielastic cross section, we focus on Eq. 49, our plane-wave expression for the latter. With this formula as our starting point, we can define

$$\sigma_L \equiv \int \, d\omega \frac{d^2 \bar{\sigma}}{d\omega d\Omega}\bigg|_{had} = \frac{1}{16\pi^2} \frac{p_f}{p_i} \, \hat{W}^{00}\left[|\mathcal{G}'_V|^2 + 2\text{Re} \, \mathcal{G}'_V \, \mathcal{F}'^*_S \, R^{0s} + |\mathcal{F}'_S|^2 \, R^{ss}\right] \tag{99}$$

where $\hat{W}^{00} \equiv \int d\omega \, W^{00}$, $R^{0s} \equiv \hat{W}^{0s}/\hat{W}^{00}$, $R^{ss} \equiv \hat{W}^{ss}/\hat{W}^{00}$ and

$$\mathcal{G}'_V \equiv \frac{\epsilon_i + \epsilon_f}{2m} \frac{Q^2}{\mathbf{q}^2} \, \mathcal{F}'_V. \tag{100}$$

The "L" subscript indicates we have dropped all transverse (*i.e.*, $\propto W^{11}$) contributions, retaining only "longitudinal" terms. We furthermore consider only isoscalar ($T = 0$) contributions since it is here that strong RPA correlations appear. These restrictions are intended to simplify the analysis by focussing exclusively on the physics of greatest interest. We recall that the isoscalar Coulomb response is roughly half of the full response. To assess the relative importance of the longitudinal isoscalar contribution to the K^+ cross sections, we observe that, for K^+N scattering from a free nucleon, the longitudinal $T = 0$ and $T = 1$ contributions are 0.999 and 0.017 mb/sr, respectively, while the corresponding transverse contributions are 0.120 and 0.210 mb/sr. This shows that the longitudinal isoscalar contribution accounts for about two thirds of the total. Thus the isoscalar longitudinal contributions to which we temporarily restrict our attention for the sake of simplicity are very significant components of the measured e^- and K^+ quantities.

Let us now consider the specific case of K^+ scattering from a free nucleon of mass M originally at rest. Then Eq. 99 can be expressed as

$$\sigma_L \rightarrow \sigma_L^{(0)} = \kappa_0 \frac{1 + \tau_0}{1 + 2\tau_0} \, |\mathcal{G}'_V \, + \mathcal{F}'_S|^2 \tag{101}$$

where we have used the fact (Eq. 24) that $W^{00} = W^{0s} = W^{ss} = (1 + \tau_0)/(1 + 2\tau_0)$ which also implies $R^{0s} = R^{ss} = 1$. In this expression we have also defined $\kappa_0 \equiv 1/16\pi^2 \cdot p_f/p_i$ and $\tau_0 \equiv Q^2/4M^2$ and have redefined $\mathcal{G}'_V$, all at the particular kinematics of this specific case.

We now modify this situation by letting $M \to M^*$. Since the kinematics change, we define

$$\alpha_1 \equiv \left(\frac{\epsilon_i + \epsilon_f^*}{2m} \frac{Q^{*2}}{\mathbf{q}^2} \right) \div \left(\frac{\epsilon_i + \epsilon_f^{(0)}}{2m} \frac{Q^{(0)2}}{\mathbf{q}^2} \right),$$

$$\beta_1 \equiv \frac{1 + \tau^*}{1 + 2\tau^*} \div \frac{1 + \tau_0}{1 + 2\tau_0},$$

$$\gamma \equiv \alpha_1^2 \cdot p_f^*/p_f^{(0)}$$

and

$$f(\alpha) \equiv \frac{1}{\alpha^2} \frac{|\alpha\mathcal{G}'_V + \mathcal{F}'_S|^2}{|\mathcal{G}'_V + \mathcal{F}'_S|^2} \tag{102}$$

where now the "starred" quantities refer to the *new* kinematics of the $M \to M^*$ case while the "zero" designation is for the mass M kinematics. We still have $R^{0s} = R^{ss} = 1$ and can write

$$\sigma_L^{(0)*} = \sigma_L^{(0)} \cdot \gamma\beta_1 \ f(\alpha_1). \tag{103}$$

Next we let $k_F \neq 0$ and write

$$\hat{W}^{00} \to \beta_2 \frac{1 + \tau_0}{1 + 2\tau_0}, \tag{104}$$

and

$$R^{0s} \to \alpha_2^{-1}. \tag{105}$$

Then, because $R^{ss} = (R^{0s})^2$ is an excellent approximation, we have

$$\sigma_L^* = \sigma_L^{(0)} \cdot \gamma\beta_2 \ f(\alpha_2). \tag{106}$$

where σ_L^* is now equal to the integrated uncorrelated nuclear matter cross section per nucleon obtained from the cross sections designated in Figures 3 and 4 by NM (Har).

Finally we consider the effects of the RPA. With

$$\hat{W}^{00} \to \beta_3 \cdot \frac{1 + \tau_0}{1 + 2\tau_0} \tag{107}$$

and

$$R^{0s} \to \alpha_3^{-1} \tag{108}$$

we find

$$\sigma_L^{RPA} = \sigma_L^{(0)} \cdot \gamma\beta_3 \ f(\alpha_3) \tag{109}$$

20

where σ_L^{RPA} is equal to the integrated uncorrelated nuclear matter cross section per nucleon designated in Figures 3 and 4 by NM (RPA). We also observe that the uncorrelated integrated longitudinal (e, e') response per nucleon; *i.e.*, the uncorrelated Coulomb sum per nucleon, is given by

$$\mathcal{S}_L^* = \beta_2 \cdot \left(\frac{1 + \tau_0}{1 + 2\tau_0} \right). \tag{110}$$

Its correlated counterpart is

$$\mathcal{S}_L^{RPA} = \beta_3 \cdot \left(\frac{1 + \tau_0}{1 + 2\tau_0} \right). \tag{111}$$

The point of this formulation is that, by examining the numerical values of γ, α_i and β_i as well as the behavior of $f(\alpha)$, we can understand the physical relationships between the K^+ cross section and the longitudinal (e, e') response.

In pursuit of this understanding we first determine that $\gamma = 0.85$ for $p_i = 700$ MeV/c and $M^*/M = 0.81$ which is the self-consistent nuclear matter value for the average density of ^{40}Ca. (Note that, because of K^+ absorption in the nuclear medium, we should use the slightly larger value of M^*/M appropriate to the lower average density at which the K^+N interaction occurs for quasielastic scattering. However, differences are small and we use the overall average density of ^{40}Ca, which is appropriate for electron scattering, in both cases so as to facilitate the following comparisons.) It remains to establish the behavior of the β_i and the α_i — or, more relevantly, the values of $f(\alpha_i)$ — as we include the effects of (i) $M^* \neq M$, (ii) $k_F \neq 0$ and (iii) RPA correlations. These behaviors are summarized in Figure 5 where we plot β_i, $f(\alpha_i)$ and $\sigma_L^{(i)}/\sigma_L^{(0)} = \gamma \beta_i f(\alpha_i)$ as they evolve from case (i) through case (iii). We see that $M^* \neq M$ causes only a very small change in β. Hence, the ratio of the corresponding Coulomb sums, $\mathcal{S}_L^{(0)*}/\mathcal{S}_L^{(0)} = \beta_1$, is nearly unity which implies that changing M^* from M, by itself, has very little consequence for electron scattering. The effect on the integrated K^+ quasielastic cross section is appreciable, however; we find $f(\alpha_1) = 0.87$. This large effect is traceable to the delicate cancellation between the first two and the third terms of Eq. 49 and the changes in the kinematic factors multiplying these terms brought about by $M^* \neq M$. Overall, taking into account the effect of γ, the K^+ cross section is reduced by 0.73 simply by letting $M^*/M \to 0.81$.

We next examine the effect of $k_F \neq 0$. The β factor does not change as the Coulomb strength is merely redistributed. However, now $R^{0s} \neq 1$ due to the Lorentz contraction of the scalar density and in consequence the delicate cancellation alluded to above is somewhat altered. We find $f(\alpha_2) = 0.93$ and the uncorrelated K^+ cross section goes up slightly so that $\sigma_L^*/\sigma_L^{(0)} = 0.78$.

We finally consider the influence of the RPA correlations. As shown in Figure 5, they cause β to drop dramatically to 0.61! This just reflects the strong RPA quenching of the Coulomb response which, as mentioned above, is a well-known feature of the RHA RPA [17]. We further observe that R^{0s} goes from 0.978 without correlations to 0.84 with them which means that the summed responses $\hat{W}^{0s}$ and $\hat{W}^{ss}$ are quenched even more strongly by the RPA than is $\hat{W}^{00}$! Indeed, $\hat{W}^{ss}$ is reduced by a factor of 0.46. This would seem to imply a *strong* quenching of the K^+ cross section. However, as is evident in Figure 5, such is not the case because $f(\alpha_3) = 1.38$, an increase which offsets the RPA quenching to

21

the degree that $\sigma_L^{(i)}/\sigma_L^{(0)}$ drops only from 0.78 to 0.71 (*i.e.*, by a factor of 0.91) when RPA effects are included. The large increase in $f(\alpha)$ in this case is due to the large reduction in R^{0s}, that is, due to *differential* quenching of time-like vector and scalar contributions in the RPA. If no such differential quenching were present, $\sigma_L^{(i)}/\sigma_L^{(0)}$ would necessarily decrease like β;*i.e.*, like the Coulomb sum. As the distinction between scalar and vector contributions is purely relativistic, it is hard to see how non-relativistic models of nuclear structure could simultaneously account for the strong quenching of the Coulomb sum and the absence of quenching in the K^+ quasielastic scattering cross section in a manner as natural as for the present relativistic model.

The preceeding analysis is based on a number of simplifying assumptions which can be tested, *e.g.*, by comparing with the results of more complete nuclear matter calculations which — as we have already established — are quite consistent with the full finite nucleus results. Figure 5 compares the ratio of the integrated nuclear matter cross sections — labelled "NM" — with the $\sigma_L^{(i)}/\sigma_L^{(0)}$ ratio discussed above. The agreement is good enough to inspire confidence in the simplified analysis.

Overall, we find that the *full* integrated RHA-RPA K^+ quasielastic cross section per (effective) nucleon which includes isoscalar transverse as well as isovector contributions *is* reduced from the (isospin averaged) K^+N cross section. For the VS representation of the K^+N amplitude, the reduction factor is 0.94 while for the mixed representation the factor is 0.82. These differences are clearly due to the different behavior of the isovector contributions, namely that they are appreciably enhanced by $M \rightarrow M^*$ in the VS representation but little changed in the VT representation. By comparison, the full integrated RHA-RPA Coulomb response per nucleon is reduced from the isospin averaged single nucleon value by a factor of 0.76. Clearly, while the K^+ reductions are less than for the Coulomb, they are not dramatically different, especially when the mixed representation is used for the former. However, it is important to observe that the reduction of the K^+ cross section is not due just to the quenching of the underlying responses but depends also on the interference effects discussed above. Most importantly, if it were not for the *differential quenching* of scalar versus time-like vector contributions which emerges naturally in our relativistic model of nuclear structure, the reduction factor for the K^+ cross section would be *much* smaller and therefore inconsistent with the K^+ quasielastic data. As it is, we have a gratifyingly accurate and consistent description of both the K^+ and (e, e') data.

VII. SUMMARY AND CONCLUSIONS

We have formulated a treatment of K^+-nucleus quasielastic scattering in a manner which parallels as closely as possible more-or-less standard treatments of e^--nucleus quasielastic scattering. The latter depends in a straightforward way on the Coulomb (or longitudinal) and transverse nuclear responses which in turn are of great importance in understanding essentials of nuclear structure. We have shown that — in the present formulation — K^+ quasielastic scattering depends on these same Dirac vector and tensor nuclear responses as well as additional ones containing Dirac *scalar* contributions. Thus, in principle, K^+ quasielastic data can supplement and extend structure information extracted from the electron data and perhaps shed light on important issues such as the strong quenching of the Coulomb sum [1,2,3].

Our treatment of the underlying K^+N interaction relies on the impulse approximation and we have been careful to spell out the connection between the K^+N amplitudes appearing in our expression for the K^+-nucleus quasielastic cross section, Eq. 49, and K^+N phase shift solutions [13]. We have also briefly summarized problems associated with on-shell ambiguities in the form of the e^-N amplitude [14] and have indicated how these problems carry over to the form of the K^+N amplitude. We rely on a meson-exchange model of the K^+N interaction [15] to justify a specific form of this interaction expressed as a "mixture" of Dirac vector and scalar invariants for the isoscalar channel and vector and tensor invariants for the isovector channel.

Our nuclear structure model is based on Quantum Hadrodynamics, a successful relativistic phenomenology of nuclear dynamics. We specifically focus on the Relativistic Hartree Approximation [16] and the RPA based on it [17,18]. This treatment takes into account the polarization of the nucleon sea in one-loop approximation and in so doing provides a unique mechanism for quenching the Coulomb response which is found to be in reasonable accord with experiment. We have given a thorough discussion of both full finite nucleus and nuclear matter calculations of the nuclear responses in the RHA-RPA. We also have indicated how to fix the *effective* nuclear densities and M^*/M values for the nuclear matter treatment of K^+ quasielastic scattering which is complicated by the absorption of the K^+ scattering waves.

We have compared our calculations with the Coulomb and transverse responses for ^{40}Ca at $|\mathbf{q}| = 500$ MeV/c [1]. We reproduce the low-ω side of the transverse response quite well, but, as is typical of "one-nucleon" models such as ours, we underestimate the response on the high-ω side, presumably due to the omission of meson-exchange-current and Δ-isobar effects. RPA effects strongly quench the Coulomb response relative to the uncorrelated results and bring about reasonable agreement with the data. This quenching can be interpreted as a screening of the nucleon charge due to polarization of the nucleon sea. Finite nucleus effects appear to be important in reproducing the details of the shape of the measured Coulomb response.

We have also shown similar calculations for the new ^{40}Ca$(K^+, K^{+\prime})$ data at the same momentum transfer [9,10]. Here the quenching due to the RPA is much less than for the Coulomb response and differences between finite nucleus and nuclear matter calculations are smaller. Agreement of the full RHA-RPA calculations with the measured cross sections is very good although the calculations slightly underestimate the data when the "mixed" representation of the K^+N amplitude is employed.

We have gone on to explain why the RPA quenching of the K^+ cross section is so much less than what is observed for the Coulomb response, a phenomenon which is all the more surprising given the dominanance of the "longitudinal isoscalar" contribution in the former which is where RPA effects occur in our model. The situation becomes even more puzzling upon observing that the *new* responses containing scalar contributions which arise in the case of K^+ scattering (see Eq. 49) are even more strongly quenched than the Coulomb response. However, careful analysis shows that this *differential quenching* of responses alters a sensitive cancellation in the expression for the K^+ cross section in such a way that the cross section is only slightly reduced. The situation is qualitatively unchanged for the full K^+ quasielastic cross section which also includes transverse isoscalar and isovector components. We note that the phenomenon of differential quenching is purely relativistic in origin and

that, without it, the calculated K^+ cross sections would be much smaller and in strong disagreement with experiment. We have concluded that our relativistic model of nuclear structure provides a gratifyingly accurate and consistent description of both K^+-nucleus and e^--nucleus quasielastic scattering.

VIII. ACKNOWLEDGEMENTS

REFERENCES

[1] Z.E. Meziani *et al.*, Phys.Rev.Lett.**52**, 2130 (1984).

[2] P. Barreau *et al.*, Nucl.Phys.**A402**, 515 (1983).

[3] G. Co', K.F. Quader, R.D. Smith and J. Wambach, Nucl.Phys.**A485**, 61 (1988).

[4] T.A. Carey, K.W. Jones, J.B. McClelland, J.M. Moss, L.B. Rees, N. Tanaka and A.D. Bacher, Phys.Rev.Lett.**53**, 144 (1984); L.B. Rees, J.M. Moss, T.A. Carey, K.W. Jones, J.B. McClelland, N. Tanaka, A.D. Bacher and H. Esbensen, Phys.Rev.**C34**, 627 (1986).

[5] O. Häusser *et al.*, Phys.Rev.Lett. **61**, 822 (1988); C. Chan *et al.*, Nucl.Phys.**A510**, 713 (1990).

[6] J.B. McClelland *et al.*, Phys.Rev.Lett.**69**, 582 (1992); X.Y. Chen *et al.*, Phys.Rev.**C47**, 2159 (1993); T.N. Taddeucci *et al.*, submitted to Phys.Rev.Lett.

[7] J. Ouyang, S. Høibråten and R.J. Peterson, Phys.Rev.**C48**, 1074 (1993); J. Wise *et al.*, Phys.Rev.**C48**, 1840 (1993).

[8] D. Marlow *et al.*, Phys.Rev.**C25**, 2619 (1982); P.B. Siegel, W.B. Kaufman and W.R. Gibbs, Phys.Rev.**C30**, 1256 (1984); R.A. Krause *et al.*, Phys.Rev.**C46**, 655 (1992).

[9] C.M. Kormanyos, R.J. Peterson, J.R. Shepard, J.E. Wise, S. Bart, R.E. Chrien, L. Lee, B.L. Clausen, J. Piekarewicz, M.B. Barakat, R.A. Michael, and T. Kishimoto, Phys.Rev.Lett.**71**, 2571 (1993).

[10] C.M. Kormanyos, R.J. Peterson, J.R. Shepard, J.E. Wise, S. Bart, R.E. Chrien, L. Lee, B.L. Clausen, J. Piekarewicz, M.B. Barakat, E.V. Hungerford, R.A. Michael, K.H. Hicks and T. Kishimoto, submitted to Phys.Rev.**C**.

[11] A.L. Fetter and J.D. Walecka, <u>Quantum Theory of Many-Particle Systems</u>, McGraw-Hill, New York, 1971.

[12] See, *e.g.*, T.W. Donnelly and J.D. Walecka, Ann. Rev. of Nucl. and Part. Sci., Vol. **25**, 329 (1975).

[13] R.A. Arndt and L. Roper, *Scattering Analyses Interactive Dial-in program* (SAID), Virginia Polytechnic Institute and State University (unpublished). We have used phase shift solution SP88 in the present work.

[14] Taber DeForest, Jr., Phys.Rev.Lett.**53**, 895 (1984)

[15] R. Büttgen, K. Holinde, A. Müller-Groeling, J. Speth and P. Wynborny, Nucl.Phys.**A506**, 586 (1990).

[16] B.D. Serot and J.D. Walecka, Adv. in Nucl.Phys.**16**, J.W. Negele and E. Vogt, eds. (Plenum, N.Y. 1986).

[17] C.J. Horowitz and J. Piekarewicz, Phys.Rev.Lett.**62**, 391 (1989); Nucl.Phys.**A511**, 461 (1990).

[18] C.E. Price, E. Rost, J.R. Shepard, and J.A. McNeil, Phys.Rev.**C45**, 1089 (1992).

[19] H.-C. Jean, J. Piekarewicz and A.G. Williams, Phys.Rev.**C49**, 1981 (1994).

FIGURES

FIG. 1. The longitudinal (e, e') response, S_L, for ^{40}Ca at $|\mathbf{q}| = 500$ MeV/c. Data are from Ref. [1]. RHA nuclear matter (NM) and finite nucleus (FN) calculations without (Har) and with (RPA) RPA correlations as descibed in the text are shown.

FIG. 2. Same as Figure 1, but for the transverse (e, e') response, S_T.

FIG. 3. The K^+ quasielastic cross section at $p_K = 703$MeV/c and $\theta_{lab} = 43$ degrees. The data are from Refs. [9,10]. RHA nuclear matter (NM) and finite nucleus (FN) calculations without (Har) and with (RPA) RPA correlations and employing the VS representation of the K^+N amplitude are shown. The calculations are normalized using $A_{eff} = 21$, the centroid of the experimentally determined range of A_{eff} for ^{40}Ca [9,10].
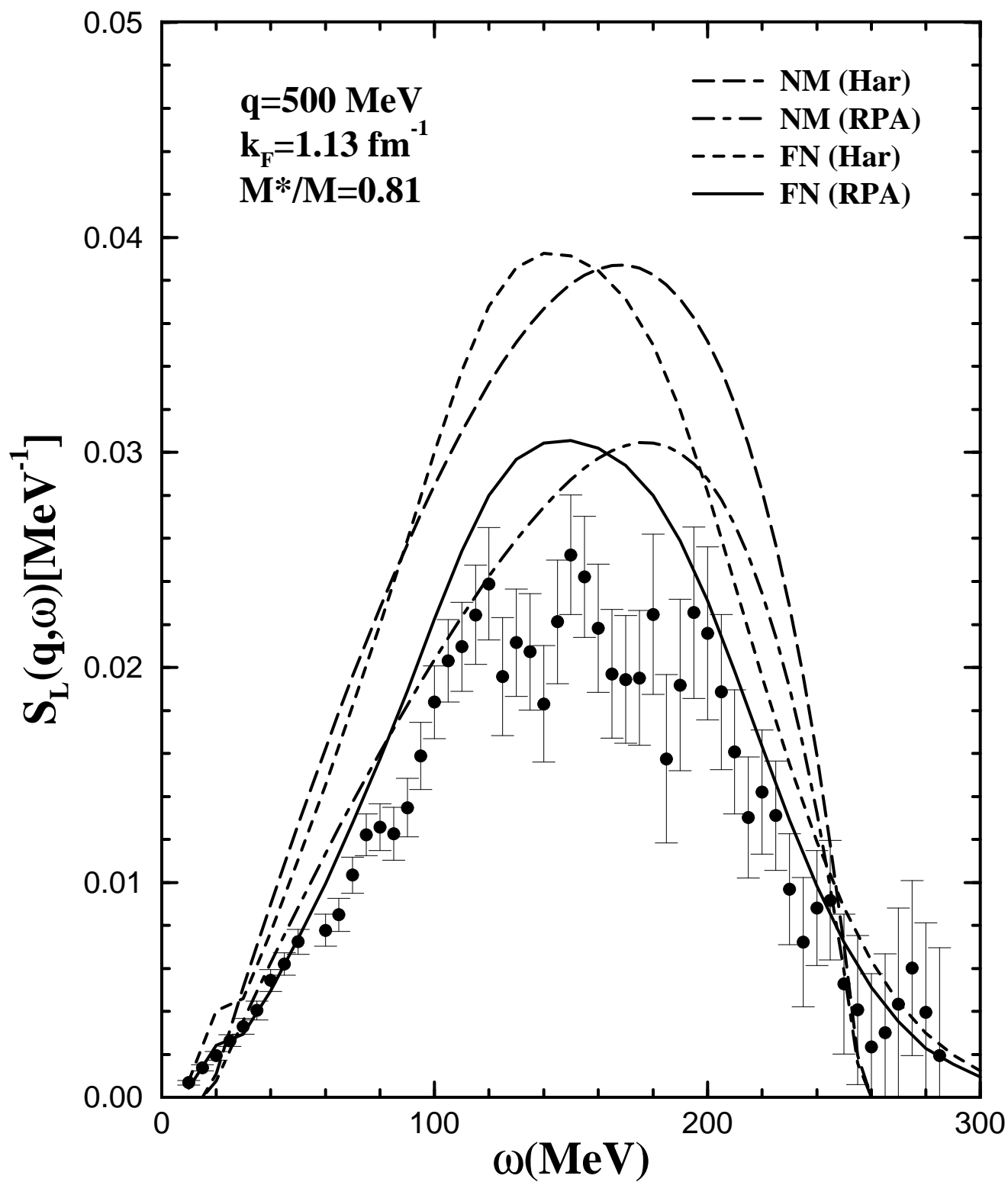

FIG. 4. Same as Figure 3 except that the mixed representation of the K^+N amplitude is used and that the calculations are normalized using $A_{eff} = 24$, the upper limit of the experimentally determined range of A_{eff} for ^{40}Ca [9,10].

FIG. 5. The evolution of the integrated longitudinal isoscalar K^+ cross section per nucleon is shown for (i) a single nucleon of mass M initially at rest, (ii) a single nucleon of mass $M^* = 0.81M$ initially at rest, (iii) a Fermi gas of nucleons of mass $M^* = 0.81M$ and Fermi momentum $k_F = 1.13$ fm^{-1} and (iv) a system like (iii) except with RPA correlations. See discussion in text.

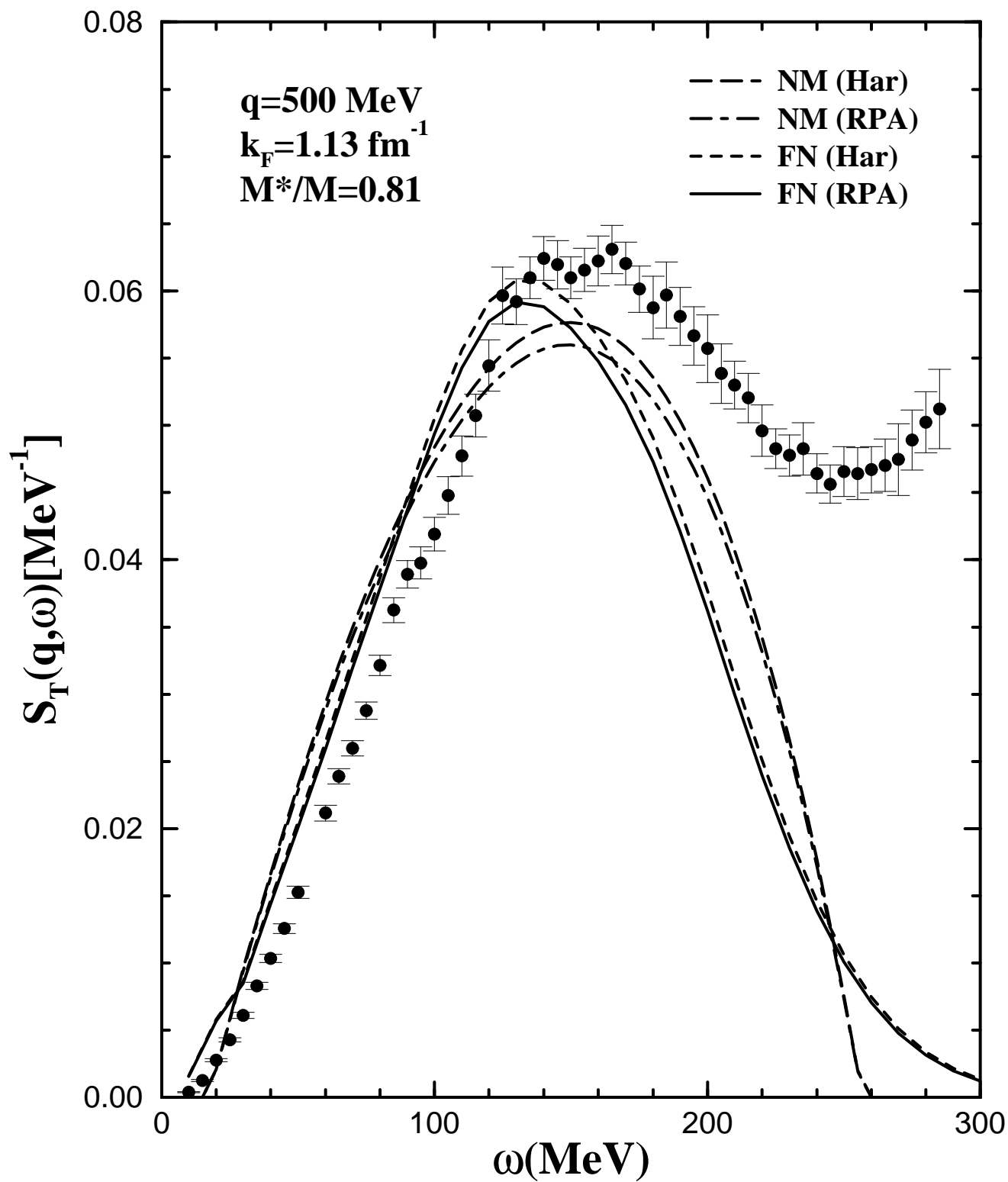This figure "fig1-1.png" is available in "png" format from:

http://arXiv.org/ps/nucl-th/9408021v1

This figure "fig1-2.png" is available in "png" format from:

http://arXiv.org/ps/nucl-th/9408021v1

^{40}Ca(e,e')

q=500 MeV
k_F=1.13 fm^{-1}
M*/M=0.81

NM (Har)
NM (RPA)
FN (Har)
FN (RPA)

This figure "fig1-3.png" is available in "png" format from:

http://arXiv.org/ps/nucl-th/9408021v1

^{40}Ca(K$^+$,K$^{+'}$)

q=500 MeV
k$_F$=1.04 fm^{-1}
M*/M=0.84
A$_{eff}$=21 [S+V]

NM (Har)
NM (RPA)
FN (Har)
FN (RPA)
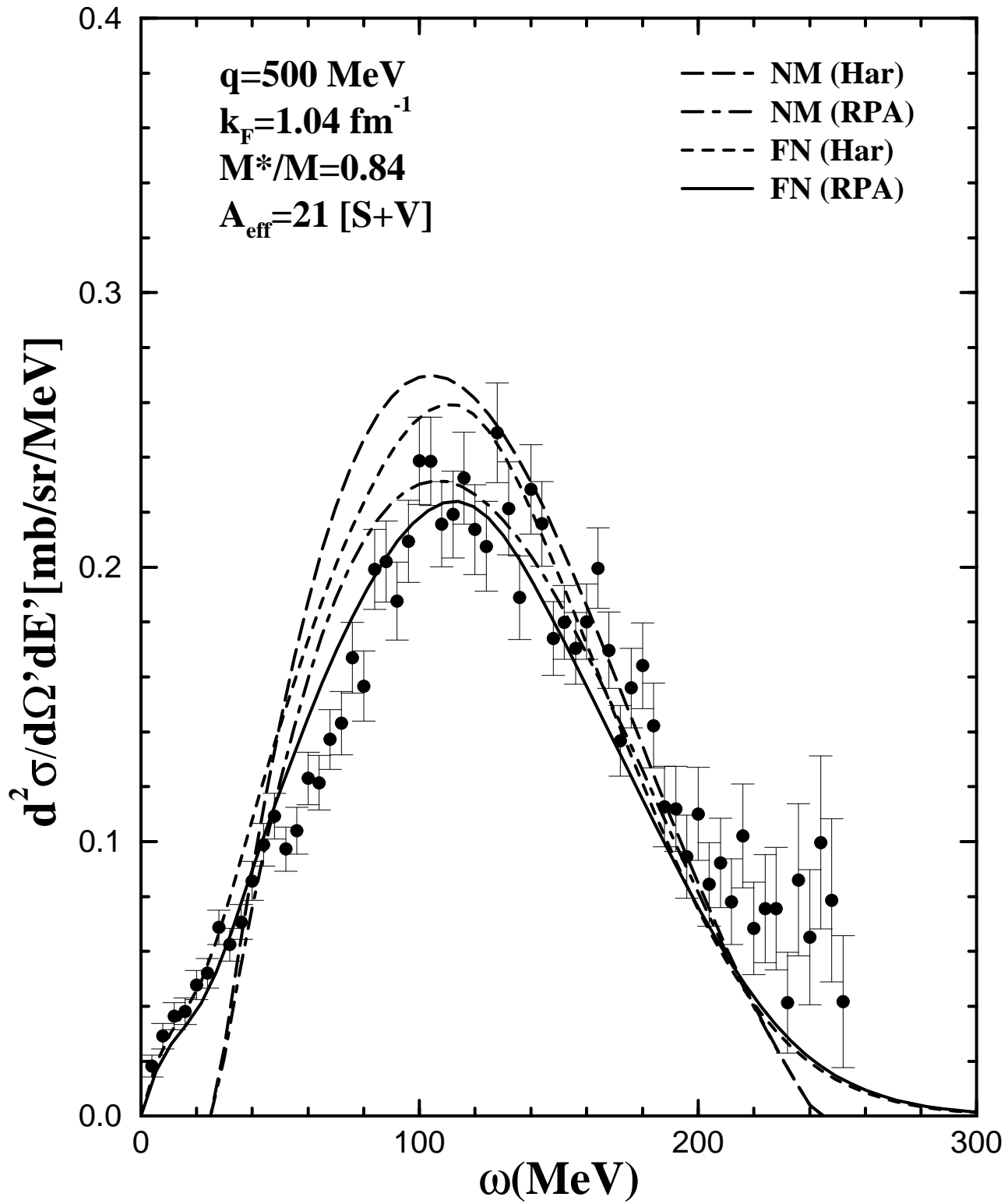
This figure "fig1-4.png" is available in "png" format from:

http://arXiv.org/ps/nucl-th/9408021v1

^{40}Ca(K$^+$,K$^{+'}$)
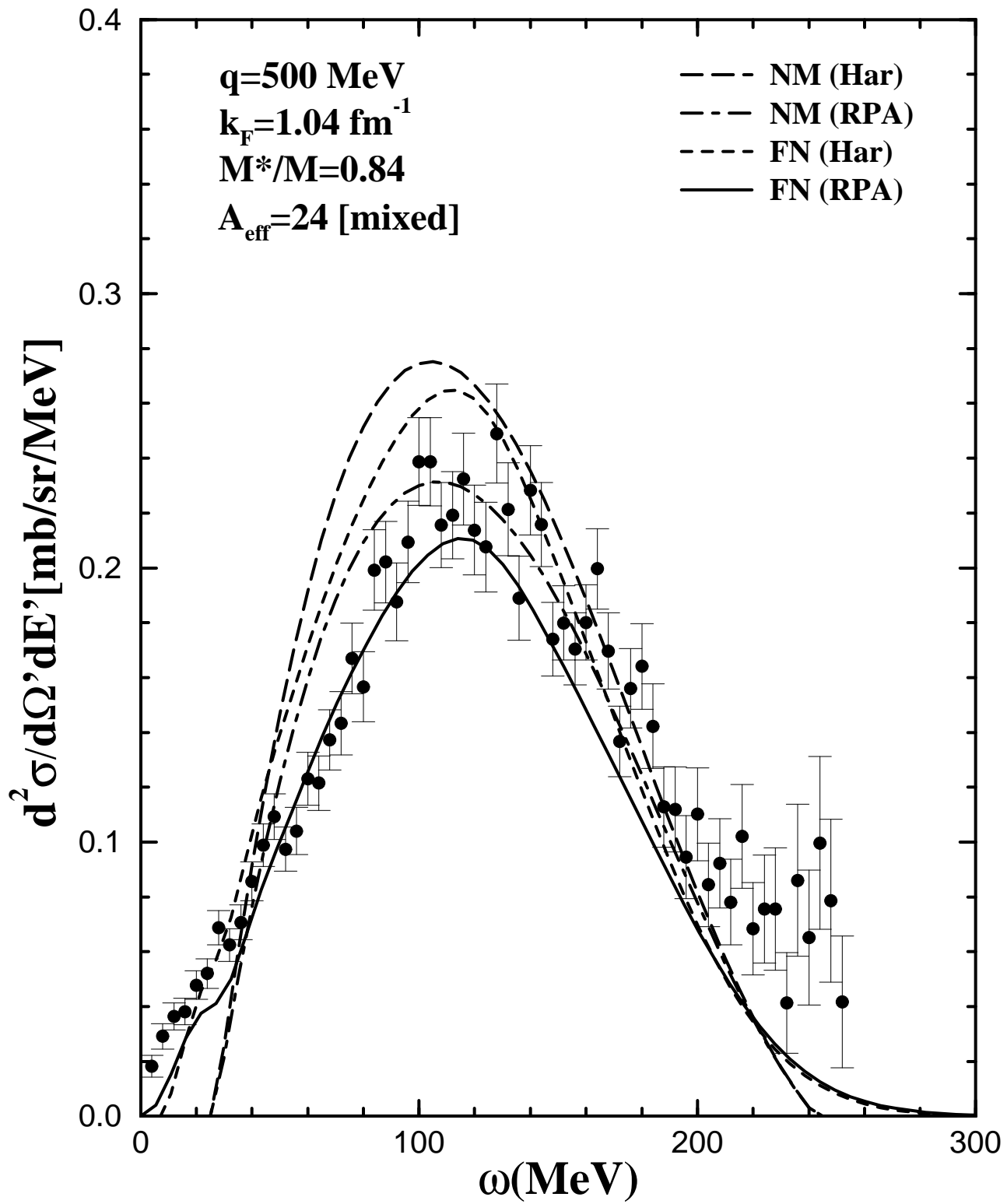
This figure "fig1-5.png" is available in "png" format from:

http://arXiv.org/ps/nucl-th/9408021v1

Evolution of K^+ Cross Section